

Quantum electrodynamic calculation of the hyperfine structure of ^3He

K. Pachucki,¹ V. A. Yerokhin,² and P. Cancio Pastor^{3,4}

¹*Faculty of Physics, University of Warsaw, Hoża 69, 00-681 Warsaw, Poland*

²*St. Petersburg State Polytechnical University, Polytekhnicheskaya 29, St. Petersburg 195251, Russia*

³*Istituto Nazionale di Ottica-CNR (INO-CNR), Via Nello Carrara 1, I-50019 Sesto Fiorentino, Italy*

⁴*European Laboratory for Non-Linear Spectroscopy (LENS) and Dipartimento di Fisica, Università di Firenze, Via N. Carrara 1, I-50019 Sesto Fiorentino, Italy*

The combined fine and hyperfine structure of the 2^3P states in ^3He is calculated within the framework of nonrelativistic quantum electrodynamics. The calculation accounts for the effects of order $m\alpha^6$ and increases the accuracy of theoretical predictions by an order of magnitude. The results obtained are in good agreement with recent spectroscopic measurements in ^3He .

PACS numbers: 31.30.Gs, 31.30.J-, 31.15.ac, 21.10.Ft

I. INTRODUCTION

Spectroscopic measurements of the helium atom have presently reached the level of accuracy at which they are sensitive to uncertainties of fundamental constants and the nuclear effects. This fact can be utilized for improving our knowledge on fundamental constants and nuclear parameters. A recent example is the independent determination of the fine structure constant α [1] made by comparison of the theoretical prediction and the experimental results for the ^4He fine structure. Good agreement of the obtained value of α with the more precise determinations [2, 3] provided a highly sensitive test of consistency of different theories across a wide range of energy scales.

Recent optical measurements in ^3He [4, 5] and ^4He [6] achieved the relative precision of about 10^{-11} and thus became sensitive to the uncertainties of the Rydberg constant and the nuclear charge radius. These experiments created a possibility for the spectroscopic determination of the nuclear charge radii of ^3He and ^4He , with a significantly higher accuracy than can be reached by the electron scattering methods [7]. Such determination is of particular interest now, in view of the discrepancy for the proton charge radius observed in the muonic hydrogen experiment [8] and the proposed follow-up experiment on the muonic helium [9]. Realization of this project requires progress in theory, namely a complete calculation of the $m\alpha^7$ corrections to the energy levels. Such calculation is difficult but probably feasible, at least for the low-lying triplet states.

While the present theory is not accurate enough to provide the nuclear charge radii of ^3He and ^4He separately, it can provide their difference δr^2 , as the isotope shift is considerably simpler to calculate than the energy levels. Two such determinations have recently been reported by experiments of the Amsterdam [4] and the Florence [5] groups, their results being in disagreement of four standard deviations. There was also the older spectroscopic value of δr^2 by Shiner *et al.* [10], which relied on the theory of the hyperfine splitting available at that time.

The main goal of the present investigation is to calculate the combined fine and hyperfine structure of the 2^3P levels of ^3He with the complete treatment of the $m\alpha^6$ corrections. The re-

sults obtained represent an order-of-magnitude improvement over the previous theory [11, 12] and are in good agreement with the experimental data available [5, 13]. The improved theory allows us to make a reevaluation of the δr^2 determination by Shiner *et al.* [10], in reasonable agreement with the Florence result [5]. We also update the previous results for the hyperfine splitting of the 2^3S state of ^3He [14], making its treatment fully consistent with that of the 2^3P states.

II. GENERAL APPROACH

The 2^3P energy level in ^3He is split by the hyperfine and fine structure effects. The hyperfine splitting is induced by the interaction between the dipole magnetic moment of the nucleus and that of the electrons, whereas the fine structure is due to the interaction between the electron spin and the electron orbital angular momentum. For heavy atoms, it is common that the hyperfine splitting (being suppressed by the electron-to-proton mass ratio) is much smaller than the fine structure splitting, and so the hyperfine and fine structure effects can be investigated separately. For the 2^3P states of ^3He , however, both effects are of the same order of magnitude and thus should be calculated together.

The general method of calculation of the combined fine and hyperfine structure is the nonrelativistic perturbation theory for quasidegenerate states. The active space of (strongly interacting) quasidegenerate states is defined as $2^3P_J^F$, where F is the total angular momentum of the atomic state and $J = 0, 1, 2$ is the electronic angular momentum. In the case of ^3He , the nuclear spin $I = 1/2$, so $F = J \pm 1/2 > 0$ and the active space consists of five levels. Note that, unlike in previous studies [11, 12, 15], we do not include the 2^1P state in the active space, as its mixing with the 2^3P levels is relatively weak. The contribution of this state is accounted for by the standard perturbation theory for non-degenerate states.

The energies of the $2^3P_J^F$ states are the eigenvalues of the 5×5 matrix of the effective Hamiltonian H , whose elements are

$$E_{J,J'}^F \equiv \langle FJM_F | H | FJ'M_F \rangle, \quad (1)$$

where M_F is the projection of the total angular momentum F . (Since the energies do not depend on M_F , it can be fixed

arbitrary.) In practical calculations, it is convenient to consider the shifts of the individual $2^3P_J^F$ levels with respect to the 2^3P centroid. In other words, we require that

$$\sum_F (2F+1) \sum_J E_{J,J}^F = 0. \quad (2)$$

In this case, all effects that do not depend on the nuclear and/or electron spin do not contribute and can be omitted in the calculations.

The matrix elements of the effective Hamiltonian (1) are obtained in this work by expansion in terms of the fine structure constant α ,

$$\begin{aligned} E_{J,J'}^F &= \langle H_{\text{fs}} \rangle_J \delta_{J,J'} + \langle H_{\text{hfs}}^{(4+)} \rangle + \langle H_{\text{hfs}}^{(6)} \rangle \\ &+ 2 \langle H_{\text{hfs}}^{(4)} \frac{1}{(E-H)'} [H_{\text{hfs}}^{(4)} + H_{\text{fs}}^{(4)}] \rangle \\ &+ \langle H_{\text{hfs}}^{(4)} \frac{1}{(E-H)'} H_{\text{hfs}}^{(4)} \rangle + \langle H_{\text{nucl}\&\text{cho}} \rangle, \end{aligned} \quad (3)$$

where H_{fs} is the effective operator responsible for the fine-structure splitting in the absence of the nuclear spin and the other terms are the nuclear-spin-dependent contributions. $H_{\text{hfs}}^{(4+)}$ is the leading hyperfine Hamiltonian with the recoil and anomalous magnetic moment additions; it is of nominal order $m\alpha^4$ and contains parts of higher-order contributions. $H_{\text{hfs}}^{(6)}$ is the effective Hamiltonian of order $m\alpha^6$ and is derived in the present work. The next two terms in Eq. (3) are the second-order corrections that also contribute to order $m\alpha^6$. $H_{\text{hfs}}^{(4)}$ is $H_{\text{hfs}}^{(4+)}$ without the recoil and anomalous magnetic moment additions, $H_{\text{fs}}^{(4)}$ is the effective Hamiltonian responsible for the leading fine-structure splitting of order $m\alpha^4$, and $H_{\text{hfs}}^{(4)}$ is the effective Hamiltonian responsible for spin independent effects of order $m\alpha^4$. Finally, $H_{\text{nucl}\&\text{cho}}$ represents the nuclear effects and the higher-order ($\sim m\alpha^7$) QED corrections proportional to the δ function at the origin. This part cannot be accurately calculated at present, because of insufficient theoretical knowledge of the nuclear structure. It will be obtained from the experiment on the ground-state hyperfine splitting in ^3He .

In order to facilitate the evaluation of the matrix elements in Eq. (3), it is convenient to factorize out their dependence on the nuclear degrees of freedom F and M_F and on the electronic angular momentum J . It can be achieved by observing that any operator contributing to Eq. (3) can be represented in terms of six basic angular-momentum operators: $(\vec{S} \cdot \vec{L})$, $(\vec{I} \cdot \vec{L})$, $(\vec{I} \cdot \vec{S})$, $(S^i S^j)^{(2)}$ $(L^i L^j)^{(2)}$, $I^i S^j (L^i L^j)^{(2)}$, and $I^i L^j (S^i S^j)^{(2)}$, where the second-order tensors are defined by $(L^i L^j)^{(2)} \equiv 1/2 L^i L^j + 1/2 L^j L^i - 1/3 \vec{L}^2 \delta^{ij}$ and the summation over the repeated indices is assumed. Since the nuclear spin of helion $I = 1/2$, there are no operators quadratic in I . So, Eq. (3) can be represented as

$$\begin{aligned} E_{J,J'}^F &= A_{\text{sl}} \langle \vec{S} \cdot \vec{L} \rangle + A_{\text{ss}} \langle (S^i S^j)^{(2)} (L^i L^j)^{(2)} \rangle \\ &+ A_{\text{s}} \langle \vec{I} \cdot \vec{S} \rangle + A_1 \langle \vec{I} \cdot \vec{L} \rangle + A_{\text{ssl}} \langle I^i S^j (L^i L^j)^{(2)} \rangle \\ &+ A_{\text{ssl}} \langle I^i L^j (S^i S^j)^{(2)} \rangle, \end{aligned} \quad (4)$$

where the constants A_i do not depend on F , M_F , J , J' , and are represented by expectation values of purely electronic operators between the spatial 2^3P wave functions. The matrix elements of the basic angular-momentum operators are calculated analytically by means of the Racah algebra and listed in Appendix A.

The first two terms in the right-hand-side of Eq. (4) do not depend on the nuclear spin and correspond to the fine structure. The fine structure splitting in the absence of the nuclear spin was investigated in our previous investigations [1, 17], so we use results obtained there.

III. LEADING HYPERFINE STRUCTURE

The leading hyperfine-structure Hamiltonian $H_{\text{hfs}}^{(4+)}$ is well known. For our purposes, it is convenient to write it in the following form,

$$\begin{aligned} H_{\text{hfs}}^{(4+)} &= \frac{m_r^3}{mM} (1 + \kappa) \alpha^4 \left[\vec{I} \cdot \vec{S} Q + \vec{I} \cdot \vec{Q} + I^i S^j Q^{ij} \right. \\ &\left. + \vec{I} \cdot \vec{S}_A Q_A + I^i S_A^j Q_A^{ij} \right], \end{aligned} \quad (5)$$

where \vec{S} and \vec{S}_A are the electron spin operators, $\vec{S} = (\vec{\sigma}_1 + \vec{\sigma}_2)/2$ and $\vec{S}_A = (\vec{\sigma}_1 - \vec{\sigma}_2)/2$, m_r is the reduced mass of the electron-nucleus system, M is the nuclear mass, and κ is the magnetic moment anomaly related to the nuclear dipole magnetic moment μ by

$$\frac{m}{M} (1 + \kappa) \equiv \frac{\mu}{\mu_B} \frac{1}{2ZI}, \quad (6)$$

where μ_B is the Bohr magneton. The electronic operators are given by (in atomic units)

$$Q = (1 + a_e) \frac{Z}{3} 4\pi [\delta^3(r_1) + \delta^3(r_2)], \quad (7)$$

$$Q_A = (1 + a_e) \frac{Z}{3} 4\pi [\delta^3(r_1) - \delta^3(r_2)], \quad (8)$$

$$\begin{aligned} \vec{Q} &= Z \left[\frac{\vec{r}_1}{r_1^3} \times \vec{p}_1 + \frac{\vec{r}_2}{r_2^3} \times \vec{p}_2 \right] \\ &+ \frac{m}{M} \frac{1 + 2\kappa}{1 + \kappa} \frac{Z}{2} \left[\frac{\vec{r}_1}{r_1^3} + \frac{\vec{r}_2}{r_2^3} \right] \times (\vec{p}_1 + \vec{p}_2), \end{aligned} \quad (9)$$

$$Q^{ij} = -(1 + a_e) \frac{Z}{2} \left[\frac{1}{r_1^3} \left(\delta^{ij} - 3 \frac{r_1^i r_1^j}{r_1^2} \right) + \frac{1}{r_2^3} \left(\delta^{ij} - 3 \frac{r_2^i r_2^j}{r_2^2} \right) \right], \quad (10)$$

$$Q_A^{ij} = -(1 + a_e) \frac{Z}{2} \left[\frac{1}{r_1^3} \left(\delta^{ij} - 3 \frac{r_1^i r_1^j}{r_1^2} \right) - \frac{1}{r_2^3} \left(\delta^{ij} - 3 \frac{r_2^i r_2^j}{r_2^2} \right) \right], \quad (11)$$

where a_e is the anomalous magnetic moment of the electron.

TABLE I: Expectation values of the $m\alpha^4$ hyperfine operators for the 2^3P state of ^3He , with the mass polarization included, in a.u. The expected numerical uncertainty is less than 1 on the last significant digit.

Q	$\langle Q \rangle$
$\frac{2Z}{3} 4\pi \delta^3(r_1)$	21.092 193
$2Z \frac{\vec{r}_1}{r_1^3} \times \vec{p}_1$	0.277 443
$Z \left(\frac{\vec{r}_1}{r_1^3} + \frac{\vec{r}_2}{r_2^3} \right) \times \vec{p}_1$	-0.060 491
$-Z \frac{1}{r_1^3} \left(\delta^{ij} - 3 \frac{r_1^i r_1^j}{r_1^2} \right)$	0.140 325

The matrix element of the Hamiltonian between the $2^3P_J^F$ states can be represented as

$$\begin{aligned} \langle H_{\text{hfs}}^{(4+)} \rangle_{JJ'}^F &= \frac{m_r^3}{mM} (1 + \kappa) \alpha^4 \left[\langle {}^3\bar{P} | Q | {}^3\bar{P} \rangle \langle \vec{I} \cdot \vec{S} \rangle \right. \\ &\quad + \frac{1}{2} \langle {}^3\bar{P} | \vec{Q} | {}^3\bar{P} \rangle \langle \vec{I} \cdot \vec{L} \rangle \\ &\quad \left. - \frac{3}{5} \langle {}^3\bar{P} | \hat{Q} | {}^3\bar{P} \rangle \langle I^i S^j (L^i L^j)^{(2)} \rangle \right], \quad (12) \end{aligned}$$

where the shorthand notations for the matrix elements of the electronic operators are

$$\langle \vec{\phi} | Q | \vec{\psi} \rangle = \langle \phi_i | Q | \psi_i \rangle, \quad (13)$$

$$\langle \vec{\phi} | \vec{Q} | \vec{\psi} \rangle = -i \epsilon^{ijk} \langle \phi_i | Q_j | \psi_k \rangle, \quad (14)$$

$$\langle \vec{\phi} | \hat{Q} | \vec{\psi} \rangle = \langle \phi_i | Q_{ij} | \psi_j \rangle, \quad (15)$$

and the spatial triplet odd P wave function is represented as

$$\psi^i(r_1, r_2, r) = r_1^i f(r_1, r_2, r) - (r_1 \leftrightarrow r_2), \quad (16)$$

with $f(r_1, r_2, r)$ being a real scalar function of r_1, r_2 , and $r \equiv |\vec{r}_1 - \vec{r}_2|$. The P -state wave function defined above is real and normalized to $\langle \vec{P} | \vec{P} \rangle = \langle P_i | P_i \rangle = 1$.

Matrix elements of the operators Q , \vec{Q} , and \hat{Q} in Eq. (12) are evaluated between the wave functions that include the mass polarization term in the nonrelativistic Hamiltonian. Numerical results for the expectation values of these operators are presented in Table I. We observe that the Fermi contact interaction yields a dominating contribution, which could be anticipated, as it comes from both $1s$ and $2p$ electrons. This also explains why the hyperfine splitting is of the same order as the fine splitting, since the latter comes mainly from the $2p$ electron.

IV. $m\alpha^6$ CORRECTIONS

Calculation of the $m\alpha^6$ contribution to the hyperfine structure of the 2^3P state is the principal objective of this work. Analogous calculation for the 2^3S_1 state have already been performed in Ref. [14]. Here we verify the calculation for the 2^3S state and extend it to the 2^3P state.

Derivation of the effective Hamiltonian to order $m\alpha^6$ for an arbitrary state of helium is given in Appendix B. The result is

$$\begin{aligned} H_{\text{hfs}}^{(6)} &= \frac{m_r^3}{mM} (1 + \kappa) \alpha^6 \left[\vec{I} \cdot \vec{S} (P_{\text{rad}} + P_{\text{nrad}}) \right. \\ &\quad \left. + \vec{I} \cdot \vec{P} + I^i S^j P^{ij} \right] \quad (17) \end{aligned}$$

where

$$P_{\text{rad}} = Z \left(\ln 2 - \frac{5}{2} \right) \frac{Z}{3} 4\pi [\delta^3(r_1) + \delta^3(r_2)], \quad (18)$$

is the effective operator induced by the radiative QED effects,

$$\begin{aligned} P_{\text{nrad}} &= \frac{Z^2}{3} \frac{1}{r_1^4} - \frac{Z}{3} p_1^2 4\pi \delta^3(r_1) \\ &\quad - Z \frac{\vec{r}}{r^3} \cdot \frac{\vec{r}_1}{r_1^3} + \frac{8}{3} \left(\ln 2 - \frac{5}{2} \right) Z^2 \pi \delta^3(r_1), \quad (19) \end{aligned}$$

$$\begin{aligned} \vec{P} &= -Z p_1^2 \frac{\vec{r}_1}{r_1^3} \times \vec{p}_1 - Z \frac{\vec{r}_1}{r_1^3} \times \vec{p}_2 - Z \left(\frac{\vec{r}_1}{r_1^3} \times \frac{\vec{r}}{r^3} \right) (\vec{r} \cdot \vec{p}_2), \quad (20) \end{aligned}$$

and

$$\begin{aligned} P^{ij} &= -\frac{Z}{2} \left(\frac{Z}{3r_1} + p_1^2 \right) \left(3 \frac{r_1^i r_1^j}{r_1^5} - \frac{\delta^{ij}}{r_1^3} \right) \\ &\quad + \frac{Z}{2} \left(3 \frac{r^j}{r^3} \frac{r_1^i}{r_1^3} - \delta^{ij} \frac{\vec{r}}{r^3} \cdot \frac{\vec{r}_1}{r_1^3} \right). \quad (21) \end{aligned}$$

It can be immediately seen that the operator P_{nrad} involves highly singular operators, whose matrix elements between the 3P functions diverge. However, the divergence cancels out if P_{nrad} is considered together with the second-order $m\alpha^6$ contribution, as is explained below.

The second-order $m\alpha^6$ correction δE_{sec} is given by

$$\delta E_{\text{sec}} = 2 \langle H_{\text{hfs}}^{(4)} \frac{1}{(E - H)'} [H_{\text{hfs}}^{(4)} + H_{\text{fs}}^{(4)}] \rangle, \quad (22)$$

where $H_{\text{hfs}}^{(4)}$ is obtained from $H_{\text{hfs}}^{(4+)}$ from Eq. (5) by dropping the electron magnetic moment anomaly a_e and the recoil part, and

$$H_{\text{hfs}}^{(4)} + H_{\text{fs}}^{(4)} = T + \vec{S} \cdot \vec{T} + S^i S^j T^{ij} + \vec{S}_A \cdot \vec{T}_A, \quad (23)$$

where $H_{\text{hfs}}^{(4)} \equiv T$ is the spin independent part of the effective Hamiltonian of order $m\alpha^4$,

$$\begin{aligned} T &= -\frac{p_1^4 + p_2^4}{8} + \frac{Z\pi}{2} [\delta^3(r_1) + \delta^3(r_2)] \\ &\quad - \frac{1}{2} p_1^i \left(\frac{\delta^{ij}}{r} + \frac{r^i r^j}{r^3} \right) p_2^j, \quad (24) \end{aligned}$$

and the remaining operators are responsible for the fine structure to order $m\alpha^4$,

$$\vec{T} = \frac{Z}{4} \left[\frac{\vec{r}_1}{r_1^3} \times \vec{p}_1 + \frac{\vec{r}_2}{r_2^3} \times \vec{p}_2 \right] + \frac{3}{4} \frac{\vec{r}}{r^3} \times (\vec{p}_2 - \vec{p}_1), \quad (25)$$

$$\vec{T}_A = \frac{Z}{4} \left[\frac{\vec{r}_1}{r_1^3} \times \vec{p}_1 - \frac{\vec{r}_2}{r_2^3} \times \vec{p}_2 \right] + \frac{1}{4} \frac{\vec{r}}{r^3} \times (\vec{p}_2 + \vec{p}_1), \quad (26)$$

TABLE II: Expectation values of the $m\alpha^6$ hyperfine operators for the 2^3P state of ^3He , in a.u. The expected numerical uncertainty is less than 1 on the last significant digit.

P	$\langle P \rangle$
P_{rad}	-76.220 978
P'_{nrad}	0.367 674
\vec{P}	-0.529 385
\hat{P}	-0.361 070

TABLE III: Individual second-order matrix elements, for different types of intermediate states sL , in a.u. The expected numerical uncertainty is less than 1 on the last significant digit, when not given explicitly.

sL	(A, B)	$\left\langle A \frac{1}{(E-H)} B \right\rangle$
3P	(Q', T')	63.531 80
	(\vec{Q}, T)	0.085 734
	(\hat{Q}, T)	0.044 830
	(Q, \vec{T})	0.030 473
	(\vec{Q}, \vec{T})	0.010 782
	(\hat{Q}, \vec{T})	-0.051 433
	(Q, \hat{T})	-0.048 826
	(\vec{Q}, \hat{T})	0.237 962
	(\hat{Q}, \hat{T})	0.114 340
1P	(Q_A, \vec{T}_A)	157.531 64
	(\hat{Q}_A, \vec{T}_A)	-1.150 (5)
3D	(\vec{Q}, \vec{T})	0.001 148
	(\vec{Q}, \hat{T})	-0.000 434
	(\hat{Q}, \vec{T})	0.020 6 (2)
	(\hat{Q}, \hat{T})	-0.000 740
1D	(\hat{Q}_A, \vec{T}_A)	0.001 8 (3)
3F	(\hat{Q}, \hat{T})	0.011 100

and

$$T^{ij} = \frac{1}{2} \frac{1}{r^3} \left(\delta^{ij} - 3 \frac{r^i r^j}{r^2} \right). \quad (27)$$

Let us now consider the sum of singular contributions,

$$\delta_{\text{sing}} E = \frac{m_r^3}{m M} (1 + \kappa) \alpha^6 \vec{I} \cdot \vec{S} \left[\langle P_{\text{nrad}} \rangle + \left\langle Q \frac{1}{(E-H)'} T + \text{h.c.} \right\rangle \right]. \quad (28)$$

While the expectation values of the operators Q and T are finite, the second-order matrix element of these operators diverges. In order to eliminate the divergences, we regularize the Coulomb electron-nucleus interaction by introducing an artificial parameter λ ,

$$\frac{Z}{r_a} \rightarrow \frac{Z}{r_a} (1 - e^{-\lambda m Z r_a}), \quad (29)$$

All other electron-nucleus interaction terms are regularized in the same way. This entails the following replacements in effective Hamiltonians,

$$4\pi Z \delta^3(r_a) \equiv -\nabla^2 \frac{Z}{r_a} \rightarrow -\nabla^2 \frac{Z}{r_a} (1 - e^{-\lambda m Z r_a}), \quad (30)$$

$$\frac{Z^2}{r_a^4} \equiv \left(\vec{\nabla} \frac{Z}{r_a} \right)^2 \rightarrow \left[\vec{\nabla} \frac{Z}{r_a} (1 - e^{-\lambda m Z r_a}) \right]^2. \quad (31)$$

Once the electron-nucleus interaction is regularized, one can in principle calculate all matrix elements and take the limit $\lambda \rightarrow \infty$. However, since matrix elements can be calculated only numerically, it is more convenient to transform the effective operators to the regular form, where λ can be taken to infinity before numerical calculations.

To this end, we transform the operators in the second-order matrix element $T \rightarrow T'$ and $Q \rightarrow Q'$ by

$$T' \equiv T - \frac{1}{4} \sum_a \left\{ \frac{Z}{r_a}, E - H \right\}, \quad (32)$$

$$Q' \equiv Q + \frac{2}{3} \sum_a \left\{ \frac{Z}{r_a}, E - H \right\}, \quad (33)$$

where $\{\dots, \dots\}$ is the commutator and the implicit λ -regularization is assumed. After this transformation, the singular part takes the form

$$\delta_{\text{sing}} E = \frac{m_r^3}{m M} (1 + \kappa) \alpha^6 \vec{I} \cdot \vec{S} \left[\langle P'_{\text{nrad}} \rangle + \left\langle Q' \frac{1}{(E-H)'} T' + \text{h.c.} \right\rangle \right] \quad (34)$$

where both the first and second order terms are separately finite and thus the limit $\lambda \rightarrow \infty$ can be evaluated analytically. The result for the regularized operator P'_{nrad} is

$$\begin{aligned}
\langle P'_{\text{nrad}} \rangle &= \frac{2}{3} \left\langle \left(E - \frac{1}{r} \right)^2 \left(\frac{Z}{r_1} + \frac{Z}{r_2} \right) + \left(E - \frac{1}{r} \right) \left(\frac{Z^2}{r_1^2} + \frac{Z^2}{r_2^2} + 4 \frac{Z}{r_1} \frac{Z}{r_2} \right) \right. \\
&\quad + 2 \frac{Z}{r_1} \frac{Z}{r_2} \left(\frac{Z}{r_1} + \frac{Z}{r_2} \right) - \left(E - \frac{1}{r} + \frac{Z}{r_2} - \frac{p_2^2}{2} \right) 4 \pi Z \delta^3(r_1) - \frac{5 Z}{4} \frac{r^i}{r^3} \left(\frac{r_1^i}{r_1^3} - \frac{r_2^i}{r_2^3} \right) \\
&\quad + p_1^i \frac{Z^2}{r_1^2} p_1^i + p_2^2 \frac{Z^2}{r_1^2} - p_2^2 \frac{Z}{r_1} p_1^2 + 2 p_2^i \frac{Z}{r_1} \left(\frac{\delta^{ij}}{r} + \frac{r^i r^j}{r^3} \right) p_1^j \left. \right\rangle \\
&\quad - \frac{1}{6} \left\langle \frac{Z}{r_1} + \frac{Z}{r_2} \right\rangle \langle 4 \pi Z [\delta^3(r_1) + \delta^3(r_2)] \rangle + \frac{4}{3} \left\langle \frac{Z}{r_1} + \frac{Z}{r_2} \right\rangle \langle T \rangle. \tag{35}
\end{aligned}$$

Matrix elements of the regularized $m\alpha^6$ Hamiltonian are obtained by

$$\begin{aligned}
\langle H_{\text{hfs}}^{(6)} \rangle &= \frac{m_r^3}{m M} (1 + \kappa) \alpha^6 \left[\langle {}^3\vec{P} | (P_{\text{rad}} + P'_{\text{nrad}}) | {}^3\vec{P} \rangle \langle \vec{I} \cdot \vec{S} \rangle \right. \\
&\quad + \frac{1}{2} \langle {}^3\vec{P} | \vec{P} | {}^3\vec{P} \rangle \langle \vec{I} \cdot \vec{L} \rangle \\
&\quad \left. - \frac{3}{5} \langle {}^3\vec{P} | \hat{P} | {}^3\vec{P} \rangle \langle I^i S^j (L^i L^j)^{(2)} \rangle \right]. \tag{36}
\end{aligned}$$

The numerical results for the expectation values of the electronic operators are listed in Table II.

The second-order $m\alpha^6$ correction [Eq. (22)] is conceptually simple but its calculation is rather involved technically. This is partly because of the coupling with intermediate states of different symmetries (3P , 1P , 3D , 1D , and 3F) and partly due to the presence of nearly singular operators. For achieving numerically stable results, some operators had to be transformed to the regular form by using the same method as for the singular part. Details of the calculation and the regularization procedure are described in Appendix C.

Numerical results for the second-order $m\alpha^6$ corrections

are presented in Table III. Note a large contribution of the 1P intermediate states, which is mainly due to the ${}^2^3P$ - 2^1P mixing. We also mention that the numerical uncertainties of the second-order corrections are completely negligible on the level of the total theoretical error.

V. SECOND-ORDER HFS CORRECTION

The fifth term in Eq. (3) is the second-order hyperfine correction. Its nominal order is $(m^2/M) \alpha^6$. However, it is enhanced by the small ${}^2^3P$ - 2^1P energy difference in the denominator, which makes it numerically significant. Rigorous calculation of this contribution is difficult because of divergences, which are canceled by the corresponding contribution from the nuclear-structure effects. In the present work, we approximate the second-order hyperfine contribution by keeping only the lowest lying ${}^1P_1^F$ intermediate state in the sum over spectrum.

The second-order hyperfine correction induces contributions to the isotope shift (i.e., to the centroid of the ${}^2^3P$ level),

$$\langle H_{\text{hfs}}^{(4)} \frac{1}{(E - H)'} H_{\text{hfs}}^{(4)} \rangle_{\text{iso}} \approx \frac{m_r^5}{m^2 M^2} (1 + \kappa)^2 \alpha^6 \frac{1}{E({}^2^3P) - E({}^2^1P)} \left[\frac{1}{4} \langle {}^2^3\vec{P} | Q_A | {}^2^1\vec{P} \rangle^2 + \frac{1}{20} \langle {}^2^3\vec{P} | \hat{Q}_A | {}^2^1\vec{P} \rangle^2 \right], \tag{37}$$

to the fine structure,

$$\begin{aligned}
\langle H_{\text{hfs}}^{(4)} \frac{1}{(E - H)'} H_{\text{hfs}}^{(4)} \rangle_{\text{fs}} &\approx \frac{m_r^5}{m^2 M^2} (1 + \kappa)^2 \alpha^6 \frac{1}{E({}^2^3P) - E({}^2^1P)} \left[\langle {}^2^3\vec{P} | Q_A | {}^2^1\vec{P} \rangle \langle {}^2^3\vec{P} | \hat{Q}_A | {}^2^1\vec{P} \rangle \langle \frac{3}{10} (S^i S^j)^{(2)} (L^i L^j)^{(2)} \rangle \right. \\
&\quad \left. + \langle {}^2^3\vec{P} | \hat{Q}_A | {}^2^1\vec{P} \rangle^2 \langle -\frac{9}{160} \vec{L} \cdot \vec{S} + \frac{21}{400} (L^i L^j)^{(2)} (S^i S^j)^{(2)} \rangle \right], \tag{38}
\end{aligned}$$

and to the hyperfine structure,

$$\begin{aligned}
\langle H_{\text{hfs}}^{(4)} \frac{1}{(E - H)'} H_{\text{hfs}}^{(4)} \rangle_{\text{hfs}} &\approx \frac{m_r^5}{m^2 M^2} (1 + \kappa)^2 \alpha^6 \frac{1}{E({}^2^3P) - E({}^2^1P)} \left[\langle {}^2^3\vec{P} | Q_A | {}^2^1\vec{P} \rangle^2 \langle -\frac{1}{2} \vec{I} \cdot \vec{S} \rangle \right. \\
&\quad + \langle {}^2^3\vec{P} | Q_A | {}^2^1\vec{P} \rangle \langle {}^2^3\vec{P} | \hat{Q}_A | {}^2^1\vec{P} \rangle \langle -\frac{3}{10} I^i S^j (L^i L^j)^{(2)} \rangle \\
&\quad \left. + \langle {}^2^3\vec{P} | \hat{Q}_A | {}^2^1\vec{P} \rangle^2 \langle -\frac{3}{40} \vec{I} \cdot \vec{L} + \frac{1}{20} \vec{I} \cdot \vec{S} + \frac{21}{200} I^i S^j (L^i L^j)^{(2)} - \frac{9}{200} I^i L^j (S^i S^j)^{(2)} \rangle \right]. \tag{39}
\end{aligned}$$

TABLE IV: Second-order hyperfine matrix elements, in a.u., all figures shown are exact. Notations are: $(A, B) = \langle 2^3P|A|2^1P \rangle \langle 2^1P|B|2^3P \rangle / [E(2^3P) - E(2^1P)]$. The expected numerical uncertainty is less than 1 on the last significant digit.

(Q_A, Q_A)	-47774.980
(Q_A, \hat{Q}_A)	249.528
(\hat{Q}_A, \hat{Q}_A)	-1.303

Numerical results for the second-order hyperfine corrections are presented in Table IV.

The approximate treatment of the second-order hyperfine contribution yields, in our opinion, the dominant uncertainty of our theoretical predictions for the hyperfine structure. It is, therefore, important to estimate the neglected part. To this end, we introduce a different approximation for the second-order hyperfine contribution, which is obtained from Eq. (39) by the following substitution

$$\frac{1}{E(2^3P) - E(2^1P)} \langle 2^3\vec{P}|Q_A|2^1\vec{P} \rangle^2 \rightarrow \sum_n \frac{1}{E(2^3P) - E(n^1P)} \langle 2^3\vec{P}|Q'_A|n^1\vec{P} \rangle^2, \quad (40)$$

where Q'_A is the regularized δ function operator given by Eq. (C20). The difference between these two approximations (of about a half percent) is used as the estimated error of the theoretical hyperfine structure.

VI. NUCLEAR-STRUCTURE CONTRIBUTION

The last term in Eq. (3) is the nuclear-structure and higher-order QED contribution. Accurate calculation of the nuclear contribution is presently not possible due to insufficient knowledge of the nuclear dynamics. However, one may claim that the dominant part of this effect comes from a local operator proportional to the δ function at the origin. Using this assumption, one can infer the nuclear-structure correction in neutral ^3He from the experimental value of the ground-state hyperfine splitting in $^3\text{He}^+$, measured very accurately by Schlüsser *et al* [16] half a century ago. This approach has been used also in the previous studies of the ^3He hyperfine structure [11, 12].

In order to infer the nuclear-structure contribution, we subtract from the $^3\text{He}^+$ experimental result the hydrogenic limit of all corrections accounted for in the previous sections. The remainder is the nuclear-structure contribution plus some (small) higher-order QED corrections. Specifically, we define the nuclear-structure and higher-order QED contribution $C_{\text{nucl\&ho}}$ as

$$E_{\text{exp}}(1s, ^3\text{He}^+) = \frac{m_r^3}{mM} (1 + \kappa) \alpha^4 \left\{ 1 + a_e + \alpha^2 \left[\frac{3}{2} Z^2 + Z \left(\ln 2 - \frac{5}{2} \right) \right] + \alpha C_{\text{nucl\&ho}} \right\} \frac{2Z}{3} \langle 4\pi\delta^3(r) \rangle, \quad (41)$$

where $E_{\text{exp}}(1s, ^3\text{He}^+)/h = 8665649.867(10)$ kHz is the experimental result of Ref. [16]. The above equation yields

$$C_{\text{nucl\&ho}} = -0.031891. \quad (42)$$

This value does not have any theoretical uncertainty (by definition) and thus is accurate to all figures given. The corresponding contribution to the hyperfine structure in neutral helium then is

$$\langle H_{\text{nucl\&ho}} \rangle = \frac{m_r^3}{mM} (1 + \kappa) \alpha^5 C_{\text{nucl\&ho}} \times \langle 2^3\vec{P} | \frac{Z}{3} 4\pi [\delta^3(r_1) + \delta^3(r_2)] | 2^3\vec{P} \rangle \langle \vec{I} \cdot \vec{S} \rangle. \quad (43)$$

VII. SMALL CORRECTIONS

Here we pick up some higher-order contributions, which are not accounted for by $C_{\text{nucl\&ho}}$ but might be relevant for comparison with experiment. Since the mixing of the 2^3P and 2^1P levels by the fine-structure operator is large, we calculate here the anomalous magnetic moment and recoil corrections to this mixing, which are of orders $\alpha^7 m^2/M$ and $\alpha^6 m^3/M^2$, respectively.

The nuclear spin dependent 2^3P - 2^1P fine-structure mixing is given by

$$\langle H_{\text{mix}} \rangle = \frac{m_r^3}{mM} (1 + \kappa) \alpha^6 \frac{m_r^2}{m^2} \frac{1}{E(2^3P) - E(2^1P)} \left[\langle 2^3\vec{P}|Q_A|2^1\vec{P} \rangle \langle 2^1\vec{P}|\vec{T}_A|2^3\vec{P} \rangle \langle \frac{1}{3} \vec{I} \cdot \vec{L} - I^i L^j (S^i S^j)^{(2)} \rangle + \langle 2^3\vec{P}|\hat{Q}_A|2^1\vec{P} \rangle \langle 2^1\vec{P}|\vec{T}_A|2^3\vec{P} \rangle \langle -\frac{1}{6} \vec{I} \cdot \vec{L} + \frac{9}{20} I^i S^j (L^i L^j)^{(2)} + \frac{1}{20} I^i L^j (S^i S^j)^{(2)} \rangle \right], \quad (44)$$

where the Q_A and \vec{T}_A operators include the anomalous mag-

netic moment and the recoil additions,

$$Q_A = (1 + a_e) \frac{Z}{3} 4\pi [\delta^3(r_1) - \delta^3(r_2)], \quad (45)$$

$$\vec{T}_A = (1 + 2a_e) \frac{Z}{4} \left[\frac{\vec{r}_1}{r_1^3} \times \vec{p}_1 - \frac{\vec{r}_2}{r_2^3} \times \vec{p}_2 \right] + \frac{1}{4} \frac{\vec{r}}{r^3} \times (\vec{p}_2 + \vec{p}_1)$$

$$+ m (1 + a_e) \frac{Z}{4} \left(\frac{\vec{r}_1}{r_1^3} - \frac{\vec{r}_2}{r_2^3} \right) \times (\vec{p}_1 + \vec{p}_2) \quad (46)$$

TABLE V: Nuclear-spin dependent fine-structure mixing matrix elements, with the anomalous magnetic moment and mass polarization (upper entry) and without (lower entry), in a.u., all figures shown are exact, $(A, B) \equiv \langle 2^3P|A|2^1P \rangle \langle 2^1P|B|2^3P \rangle / [E(2^3P) - E(2^1P)]$. The expected numerical uncertainty is less than 1 on the last significant digit.

(Q_A, \vec{T}_A)	156.1127
	155.9034
(\hat{Q}_A, \vec{T}_A)	-0.81535
	-0.81428

and the matrix elements are calculated between the wave functions that include the mass polarization correction.

The higher-order mixing contribution is obtained from Eq. (44) after subtracting the part that is already accounted for [namely, the $n = 2$ term in Eq. (C6)]. Numerical results for the corresponding matrix elements are given in Table V. The recoil correction is due to both the the mass polarization and the recoil addition to T_A . Further corrections to this mixing (e.g., those coming from higher-order relativistic corrections) are not known and contribute to the uncertainty of final results.

VIII. RESULTS AND DISCUSSION

In this section we present the total theoretical predictions for the mixed fine and hyperfine structure of the 2^3P states in ^3He . The numerical values of nuclear parameters used in the calculations are [18]

$$\mu/\mu_B = -1.158\,740\,958(14) \cdot 10^{-3}, \quad (47)$$

$$m/M = 1.819\,543\,0761(17) \cdot 10^{-4}. \quad (48)$$

The conversion factors relevant for this work are

$$\frac{m_r^3}{mM} (1 + \kappa) \alpha^4 = -202\,887.3247 \text{ kHz} \times h, \quad (49)$$

$$\frac{m_r^3}{mM} (1 + \kappa) \alpha^6 = -10.8040 \text{ kHz} \times h, \quad (50)$$

$$\frac{m_r^5}{m^2 M^2} (1 + \kappa)^2 \alpha^6 = 0.0063 \text{ kHz} \times h, \quad (51)$$

where h is the Planck constant.

The fine structure splitting in the absence of the nuclear spin was calculated in our previous investigations [1, 17], with numerical results reported for ^4He . In this work, we reevaluate all nuclear-mass-dependent corrections to the fine structure, in order to extend our calculation to ^3He . The numerical results for the 2^3P_J levels of ^3He are

$$\langle H_{\text{fs}} \rangle_{J=0} = \frac{h}{9} (8 f_{01} + 5 f_{12}), \quad (52)$$

$$\langle H_{\text{fs}} \rangle_{J=1} = \frac{h}{9} (-f_{01} + 5 f_{12}), \quad (53)$$

$$\langle H_{\text{fs}} \rangle_{J=2} = \frac{h}{9} (-f_{01} - 4 f_{12}), \quad (54)$$

TABLE VI: Theoretical results for individual $2^3P_J^F$ levels in ^3He , relative to the 2^3P centroid energy, in comparison with available experimental data, in kHz. The first error of the theoretical values is the uncertainty due to the hyperfine structure and the second error is the uncertainty due to the fine structure.

$2^3P_0^{F=1/2}$	27 923 393.7 (0.2)(2.5)	
	27 923 394.7 (2.2)	Smiciklas [13]
	27 923 398.3 (1.9)	Cancio <i>et al.</i> [5]
$2^3P_2^{F=3/2}$	498 547.3 (1.4)(0.4)	
	498 543.7 (2.1)	Smiciklas [13]
	498 547.3 (2.1)	Cancio <i>et al.</i> [5]
$2^3P_1^{F=1/2}$	-169 462.2 (0.5)(0.8)	
	-169 463.3 (1.7)	Smiciklas [13]
	-169 460.2 (1.8)	Cancio <i>et al.</i> [5]
$2^3P_1^{F=3/2}$	-4 681 676.3 (0.7)(0.2)	
	-4 681 676.3 (1.5)	Smiciklas [13]
	-4 681 672.1 (1.6)	Cancio <i>et al.</i> [5]
$2^3P_2^{F=5/2}$	-6 462 557.8 (0.7)(1.0)	
	-6 462 555.3 (1.5)	Smiciklas [13]
	-6 462 562.8 (1.6)	Cancio <i>et al.</i> [5]

where

$$f_{01} = 29\,616\,676.5 (1.7) \text{ kHz}, \quad (55)$$

$$f_{12} = 2\,292\,167.6 (1.7) \text{ kHz}. \quad (56)$$

We now have all contributions to the elements of the Hamiltonian matrix $E_{J,J'}^F$ in Eq. (3). Diagonalizing the matrix, we obtain the positions of the energy levels of the $2^3P_J^F$ states in ^3He , relative to the centroid of the 2^3P level. The numerical results are listed in Table VI for the individual energy levels and in Table VII for the transitions between the fine and hyperfine levels. Our theoretical values have two uncertainties, the first one being due to the hyperfine effects and the second one, due to the fine-structure effects. The nuclear-spin dependent effects are calculated with an accuracy of about 1 kHz (and even better in some cases). This accuracy is limited mainly by the incomplete treatment of the second-order hyperfine correction. The second uncertainty of the theoretical energies is due to the fine-structure effects. It comes from the 1.7 kHz error of f_{01} and f_{12} in Eqs. (55) and (56), which is exactly the same as for the fine structure in ^4He . Interestingly, the sensitivity of different levels to the error of the fine-structure effects is very much different, varying from 0.2 kHz for the $2^3P_1^{3/2}$ level to 2.5 kHz for $2^3P_0^{1/2}$. As could be expected, the transitions between the levels with the same value of J are less sensitive to the error of the fine-structure effects than the $J - J'$ transitions.

The present theoretical results can be compared with the experiment by Smiciklas [13] and with our recently reported absolute frequency measurements of the 2^3S-2^3P transitions [5]. The latter experiment was carried out by using the optical frequency comb assisted multi-resonant precision spectroscopy [19] and by measuring simultaneously both optical

TABLE VII: Experimental and theoretical hyperfine transitions, in kHz. The first error in the theoretical prediction is the uncertainty due to the hyperfine splitting and the second error is the uncertainty due to the fine-structure splitting.

$(J, F) - (J', F')$	Value	Reference
$(0, 1/2) - (1, 1/2)$	28 092 855.9 (0.5) (1.7)	
	28 092 870 (60)	Morton <i>et al.</i> [11]
	28 092 858 (3)	Smiciklas [13]
	28 092 858.6 (2.1) ^a	Cancio <i>et al.</i> [5]
$(0, 1/2) - (2, 3/2)$	27 424 846.4 (1.4) (2.9)	
	27 424 837 (12)	Wu&Drake [12]
	27 424 851.0 (3.0)	Cancio <i>et al.</i> [5]
$(2, 3/2) - (1, 1/2)$	668 009.5 (1.4) (1.2)	
	668 033 (9)	Wu&Drake [12]
	668 007 (3)	Smiciklas [13]
	668 007.5 (3.2)	Cancio <i>et al.</i> [5]
$(1, 3/2) - (2, 5/2)$	1 780 881.5 (1.0) (1.2)	
	1 780 880 (1)	Wu&Drake [12]
	1 780 879 (3)	Smiciklas [13]
	1 780 890.7(3.5)	Cancio <i>et al.</i> [5]
$(1, 1/2) - (1, 3/2)$	4 512 214.1 (0.8) (0.5)	
	4 512 191 (12)	Wu&Drake [12]
	4 512 213 (3)	Smiciklas [13]
	4 512 211.9 (2.7)	Cancio <i>et al.</i> [5]
$(2, 3/2) - (2, 5/2)$	6 961 105.1 (1.5) (0.5)	

^aAveraged value of the two differences between the measured optical transitions.

and microwave hyperfine transition frequencies. Agreement found between the microwave frequencies and the difference of the optical transition frequencies was used as a confirmation of the obtained experimental results. Comparison of the two independent measurements (see Table VII) shows good agreement in all cases except for the $P_1^{3/2}$ - $P_2^{5/2}$ transition.

The experimental values for individual energy levels listed in Table VI are obtained from the transition energies reported in the original references [5, 13] by using the definition of the centroid [Eq. (2)] and the experimental hyperfine shift of the 2^3S state [16]. We observe that theoretical and experimental results are at the same level of accuracy of about 2-3 kHz and in very good agreement with each other. It can be concluded that our calculation of the $m\alpha^6$ correction represented an important advance over the previous theory [11, 12] and significantly improved agreement between theory and the experiment.

Table VIII shows our numerical results for the hyperfine splitting of the 2^3S state of ^3He . The results listed represent an update of the calculation described in detail in Ref. [14]. As compared to that work, we have (i) slightly improved the numerical accuracy and (ii) made the treatment of the second-order hyperfine and the nuclear-structure contributions to be fully consistent with that for the 2^3P states. The uncertainty of the theoretical prediction comes from the second-order hy-

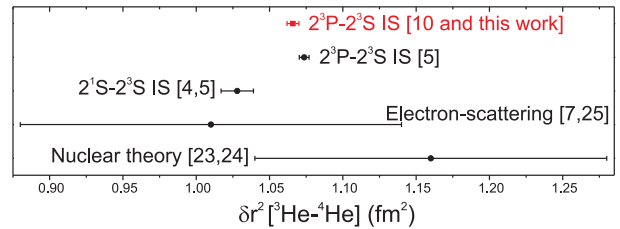


FIG. 1: (Color online) Different determinations of the difference of the squared nuclear charge radii of ^3He and ^4He .

TABLE VIII: Hyperfine splitting of the 2^3S state of ^3He , in kHz.

$H^{(4+)}$	6 740 451.46
$H^{(6)}$	-1 313.99
$(H_{\text{hfs}}^{(4)}, H_{\text{hfs}}^{(4)} + H_{\text{fs}}^{(4)})$	2 189.81
$(H_{\text{hfs}}^{(4)}, H_{\text{hfs}}^{(4)})$	-60.52 ± 1.7
$H_{\text{nucl\&ho}}$	-1 566.83
Total	$6 739 699.93 \pm 1.7$
Experiment [20]	$6 739 701.177 (16)$

perfine correction and was estimated in the same way as for the 2^3P state. Very good agreement of the 2^3S theoretical result with the experimental value [16] gives us additional confidence in our estimation of errors for the 2^3P state.

Having calculated the hyperfine and fine structure of the 2^3P levels, we are now in a position to obtain an improved determination of ^3He - ^4He nuclear charge radii difference δr^2 from the isotope shift measurement by Shiner *et al.* [10]. In order to extract δr^2 from the measured energy difference, $E(^3\text{He}, 2^3P_0^{1/2} - 2^3S_1^{3/2}) - E(^4\text{He}, 2^3P_2 - 2^3S_1)$, we subtract the experimental hyperfine shift of the 2^3S state [16], the theoretical shift of the $2^3P_0^{1/2}$ level with respect to the centroid energy (obtained in this work), the theoretical fine shift of the 2^3P_2 level with respect to the centroid [1], and the theoretical isotope shift of the centroids for the point nucleus [5] (see Table IX). The remainder δE comes from the finite nuclear size effect and is proportional to the difference of the mean square charge radii, $\delta E = C \delta r^2$, where coefficient C is evaluated in this work to be $C = -1212.2(1)$ kHz/fm². The resulting value

$$\delta r^2 \equiv r^2(^3\text{He}) - r^2(^4\text{He}) = 1.066(4) \text{ fm}^2 \quad (57)$$

is in reasonable agreement with the result by Cancio *et al.* [5], $\delta r^2 = 1.074(3)$ fm², and in significant disagreement with the result of Ref. [4] (updated in Ref. [5] by recalculation of the isotope shift), $\delta r^2 = 1.028(11)$ fm². Figure 1 shows graphically the comparison of different determinations of δr^2 , including the results from nuclear theory [23, 24] and from nuclear electron-scattering measurements [7, 25].

TABLE IX: Determination of the difference of the mean square nuclear charge radii δr^2 of ${}^3\text{He}$ and ${}^4\text{He}$ from the measurement by Shiner *et al.* [10]. The remainder δE is proportional to δr^2 , $\delta E = C \delta r^2$, with $C = -1212.2(1)$ kHz/fm², see text for details. Units are kHz.

$E({}^3\text{He}, 2^3P_0^{1/2} - 2^3S_1^{3/2}) - E({}^4\text{He}, 2^3P_2 - 2^3S_1)$	810 599.(3.)	Experiment [10]
$\delta E_{\text{hfs}}(2^3S_1^{3/2})$	-2 246 567.059(5)	Experiment [16]
$\delta E_{\text{fs}}(2^3P_2)$	-4 309 074.2(1.7)	Theory, [1] and this work, Eq. (54)
$-\delta E_{\text{hfs}}(2^3P_0^{1/2})$	-27 923 393.7 (1.7)	Theory, this work, Table VI
$-\delta E_{\text{iso}}(2^3P - 2^3S)$ (point nucleus)	33 667 143.2(3.9)	Theory [5]
δE	-1 292.8(5.2)	

IX. SUMMARY

In summary, we have calculated the mixed hyperfine and fine structure of the 2^3P states of ${}^3\text{He}$. Our investigation advances the previous theory by a complete calculation of the $m\alpha^6$ correction, which leads to an order-of-magnitude improvement in accuracy. Theoretical predictions for most of the transitions are accurate to better than 2 kHz. The $2^3P_1^{1/2} - 2^3P_1^{3/2}$ transition is calculated up to 0.9 kHz, which is currently the most precise theoretical result for the helium transitions. Both the hyperfine and fine-structure transitions are in good agreement with measurements by Cancio *et al.* [5] and by Smiciklas [13].

Since the present theoretical accuracy for the fine-structure transitions in ${}^3\text{He}$ is comparable to that for ${}^4\text{He}$, one can in principle use the ${}^3\text{He}$ spectroscopy for the determination of the fine structure constant α , as in was done for ${}^4\text{He}$ in Ref. [1]. However, such determination does not bring much

advantage at present, since the experimental accuracy for ${}^3\text{He}$ is lower than for ${}^4\text{He}$ [21, 22]. Because of this, we do not determine α from the ${}^3\text{He}$ transitions in this work. However, if the experimental precision of the ${}^3\text{He}$ hyperfine structure is improved to the sub-kHz level, one will be able to use these results for the spectropic determination of the fine structure constant.

Another application of the hyperfine structure measurements in ${}^3\text{He}$ might be determination of the dipole magnetic moment of helion. The principal problem here is that the present theory obtains the nuclear-structure contribution from the experimental value of the hyperfine splitting in ${}^3\text{He}^+$. This greatly reduces the sensitivity of the final theoretical prediction on the nuclear magnetic moment. Our calculation shows that at present, the hyperfine structure of ${}^3\text{He}$ allows for determination of the dipole magnetic moment of helion with an accuracy of about 5×10^{-5} only.

-
- [1] K. Pachucki and V. A. Yerokhin, Phys. Rev. Lett. **104**, 070403 (2010).
- [2] D. Hanneke, S. Fogwell, and G. Gabrielse, Phys. Rev. Lett. **100**, 120801 (2008).
- [3] R. Bouchendira, P. Cladé, S. Guellati-Khélifa, F. Nez, and F. Biraben, Phys. Rev. Lett. **106**, 080801 (2011).
- [4] R. van Rooij, J. S. Borbely, J. Simonet, M. Hoogerland, K. S. E. Eikema, R. A. Rozendaal, and W. Vassen, Science **333**, 196 (2011).
- [5] P. Cancio Pastor, L. Consolino, G. Giusfredi, P. De Natale, M. Inguscio, V. A. Yerokhin, and K. Pachucki, Phys. Rev. Lett. **108**, 143001 (2012).
- [6] P. Cancio Pastor *et al.* Phys. Rev. Lett. **92**, 023001 (2004), [(E) *ibid* **97**, 139903 (2006)].
- [7] I. Sick, Lect. Notes Phys. **745**, 57 (2008).
- [8] R. Pohl *et al.*, Nature (London) **466**, 213 (2010).
- [9] A. Antognini *et al.*, Can. J. Phys. **89**, 47 (2011).
- [10] D. Shiner, R. Dixon, and V. Vedantham, Phys. Rev. Lett. **74**, 3553 (1995).
- [11] D. Morton, Q. Wu, and G. W. F. Drake, Phys. Rev. A **73**, 034502 (2006).
- [12] Q. Wu and G. W. F. Drake, J. Phys. B **40**, 393 (2007).
- [13] M. Smiciklas, Master thesis, University of North Texas, unpublished, 2003; arXiv:physics/1203.2830.
- [14] K. Pachucki, J. Phys. B **34**, 3357 (2001).
- [15] F. Marin, F. Minardi, F. S. Pavone, M. Inguscio, and G. W. F. Drake, Z. Phys. D **32**, 285 (1995).
- [16] H. A. Schlusser, E. N. Fortson, and H. G. Dehmelt, Phys. Rev. **187**, 5 (1969), [(E) Phys. Rev. A **2**, 1612 (1970)].
- [17] K. Pachucki and V. A. Yerokhin, Phys. Rev. A **79**, 062516 (2009), [*ibid.* **80**, 019902(E) (2009); *ibid.* **81**, 039903(E) (2010)].
- [18] CODATA internationally recommended values of the fundamental physical constants, <http://physics.nist.gov/cuu/Constants>.
- [19] L. Consolino *et al.* Opt. Express **19**, 3155 (2011).
- [20] S. D. Rosner and F. M. Pipkin, Phys. Rev. A **1**, 571 (1970), [(E) Phys. Rev. A **3**, 521 (1971)].
- [21] J. S. Borbely, M. C. George, L. D. Lombardi, M. Weel, D. W. Fitzakerley, and E. A. Hessels, Phys. Rev. A **79**, 0605030(R) (2009).
- [22] M. Smiciklas and D. Shiner, Phys. Rev. Lett. **105**, 123001 (2010).
- [23] G. Drake, W. Nörtershäuser, and Z.-C. Yan, Can. J. Phys. **83**, 311 (2005).
- [24] I. Sick, Phys. Rev. C **77**, 041302 (2008).
- [25] A. Kievsky *et al.* J. Phys. G **35**, 063101 (2008).
- [26] D. A. Varshalovich, A. N. Moskalev, and V. K. Khersonskii, *Quantum Theory of Angular Momentum*, World Scientific, Singapore, 1988.
-

Appendix A: Angular-momentum matrix elements

In this section we calculate the matrix elements of the basic angular-momentum operators that are relevant for the present work. The angular-momentum algebra is conveniently done with formulas from Ref. [26]. The results are

$$\begin{aligned} \langle FIJLSM_F | \vec{I} \cdot \vec{S} | FIJ'L'S'M_F \rangle &= (-1)^{I+J+F} \begin{Bmatrix} I & J & F \\ J' & I & 1 \end{Bmatrix} \sqrt{I(I+1)(2I+1)} \\ &\times \delta_{L,L'} \delta_{S,S'} (-1)^{L+S+J+1} \sqrt{S(S+1)(2S+1)(2J+1)(2J'+1)} \begin{Bmatrix} S & L & J' \\ J & 1 & S \end{Bmatrix}, \end{aligned} \quad (\text{A1})$$

$$\begin{aligned} \langle FIJLSM_F | \vec{I} \cdot \vec{L} | FIJ'L'S'M_F \rangle &= (-1)^{I+J+F} \begin{Bmatrix} I & J & F \\ J' & I & 1 \end{Bmatrix} \sqrt{I(I+1)(2I+1)} \\ &\times \delta_{L,L'} \delta_{S,S'} (-1)^{L+S+J'+1} \sqrt{L(L+1)(2L+1)(2J+1)(2J'+1)} \begin{Bmatrix} L & S & J \\ J' & 1 & L \end{Bmatrix}, \end{aligned} \quad (\text{A2})$$

$$\langle I^i S^j (L^i L^j)^{(2)} \rangle = \frac{1}{4} [J(J+1) + J'(J'+1) - 2L(L+1) - 2S(S+1)] \langle \vec{I} \cdot \vec{L} \rangle - \frac{1}{3} L(L+1) \langle \vec{I} \cdot \vec{S} \rangle, \quad (\text{A3})$$

$$\langle I^i L^j (S^i S^j)^{(2)} \rangle = \frac{1}{4} [J(J+1) + J'(J'+1) - 2L(L+1) - 2S(S+1)] \langle \vec{I} \cdot \vec{S} \rangle - \frac{1}{3} S(S+1) \langle \vec{I} \cdot \vec{L} \rangle, \quad (\text{A4})$$

$$\langle (S^i S^j)^{(2)} (L^i L^j)^{(2)} \rangle = \langle \vec{L} \cdot \vec{S} \rangle^2 + \frac{1}{2} \langle \vec{L} \cdot \vec{S} \rangle - \frac{L(L+1)S(S+1)}{3}. \quad (\text{A5})$$

Appendix B: Derivation of $H_{\text{hfs}}^{(6)}$

We start with the Breit Hamiltonian H_{BP} of the atomic system in the external magnetic field,

$$H_{BP} = \sum_a H_a + \sum_{a,b;a>b} H_{ab} \quad (\text{B1})$$

$$\begin{aligned} H_a &= \frac{\vec{\pi}_a^2}{2m} - \frac{Z\alpha}{r_a} - \frac{e}{2m} \vec{\sigma}_a \cdot \vec{B}_a - \frac{\vec{\pi}_a^4}{8m^3} + \frac{\pi Z\alpha}{2m^2} \delta^3(r_a) + \frac{Z\alpha}{4m^2} \vec{\sigma}_a \cdot \frac{\vec{r}_a}{r_a^3} \times \vec{\pi}_a \\ &+ \frac{e}{8m^3} (\vec{\sigma}_a \cdot \vec{B}_a \vec{\pi}_a^2 + \vec{\pi}_a^2 \vec{\sigma}_a \cdot \vec{B}_a), \end{aligned} \quad (\text{B2})$$

$$\begin{aligned} H_{ab} &= \frac{\alpha}{r_{ab}} + \frac{\pi\alpha}{m^2} \delta^3(r_{ab}) - \frac{\alpha}{2m^2} \pi_a^i \left(\frac{\delta^{ij}}{r_{ab}} + \frac{r_{ab}^i r_{ab}^j}{r_{ab}^2} \right) \pi_b^j \\ &+ \frac{\alpha}{4m^2 r_{ab}^3} [\vec{\sigma}_a \cdot \vec{r}_{ab} \times (2\vec{\pi}_b - \vec{\pi}_a) - \vec{\sigma}_b \cdot \vec{r}_{ab} \times (2\vec{\pi}_a - \vec{\pi}_b)] \\ &+ \frac{\alpha}{4m^2} \frac{\sigma_a^i \sigma_b^j}{r_{ab}^3} \left(\delta^{ij} - 3 \frac{r_{ab}^i r_{ab}^j}{r_{ab}^2} \right), \end{aligned} \quad (\text{B3})$$

where $\vec{\pi} = \vec{p} - e\vec{A}$. Magnetic fields \vec{A} and \vec{B} induced by the nuclear magnetic moment are

$$e\vec{A}(\vec{r}) = \frac{e}{4\pi} \vec{\mu} \times \frac{\vec{r}}{r^3} = -Z\alpha \frac{(1+\kappa)}{M} \vec{I} \times \frac{\vec{r}}{r^3}, \quad (\text{B4})$$

$$e\vec{B}^i(\vec{r}) = (\vec{\nabla} \times \vec{A})^i = -Z\alpha \frac{(1+\kappa)}{M} \frac{8\pi}{3} \delta^3(r) I^i + Z\alpha \frac{(1+\kappa)}{M} \frac{1}{r^3} \left(\delta^{ij} - 3 \frac{r^i r^j}{r^2} \right) I^j. \quad (\text{B5})$$

The leading-order interaction between the nuclear spin \vec{I} and the electron spin $\vec{\sigma}_a$ is obtained from the nonrelativistic terms $1/2m \vec{\pi}_a^2$ and $e/2m \vec{\sigma}_a \cdot \vec{B}_a$, yielding

$$H_{\text{hfs}}^{(4)} = - \sum_a \left[\frac{e}{m} \vec{p}_a \cdot \vec{A}(\vec{r}_a) - \frac{e}{2m} \vec{\sigma}_a \cdot \vec{B}(\vec{r}_a) \right], \quad (\text{B6})$$

in agreement with Eq. (5). The relativistic correction to the hyperfine interaction is similarly obtained from the relativistic terms in the Breit Hamiltonian H_{BP} ,

$$H_{\text{hfs}}^{(6)} = \sum_a \frac{Z\alpha}{4m^2} \vec{\sigma}_a \cdot \frac{\vec{r}_a}{r_a^3} \times [-e\vec{A}(\vec{r}_a)] + \frac{e}{8m^3} (\vec{\sigma}_a \cdot \vec{B}_a \vec{p}_a^2 + \vec{p}_a^2 \vec{\sigma}_a \cdot \vec{B}_a) \\ + \sum_{a,b;a \neq b} \frac{\alpha}{4m^2 r_{ab}^3} \vec{\sigma}_a \cdot \vec{r}_{ab} \times [-2e\vec{A}(\vec{r}_b) + e\vec{A}(\vec{r}_a)] \quad (\text{B7})$$

$$+ \frac{e}{4m^3} \sum_a [\vec{p}_a^2 \vec{p}_a \cdot \vec{A}(\vec{r}_a) + \vec{p}_a \cdot \vec{A}(\vec{r}_a) \vec{p}_a^2] - \sum_{a \neq b} \frac{\alpha}{2m^2} p_a^i \left(\frac{\delta^{ij}}{r_{ab}} + \frac{r_{ab}^i r_{ab}^j}{r_{ab}^3} \right) [-eA^j(\vec{r}_b)]. \quad (\text{B8})$$

Using \vec{A} and \vec{B} from Eqs. (B4) and (B5), we derive Eq. (17).

Appendix C: Second order matrix elements

The second-order $m\alpha^6$ correction δE_{sec} [see Eq. (22)] is split into several parts in accordance with the symmetry of the intermediate states,

$$\delta E_{\text{sec}} = \frac{m_r^3}{mM} (1 + \kappa) \alpha^6 \left[\delta E_{\text{sing}}(^3P) + \delta E_{\text{reg}}(^3P) + \delta E(^1P) + \delta E(^3D) + \delta E(^1D) + \delta E(^3F) \right]. \quad (\text{C1})$$

The angular momentum algebra for different intermediate states is simple but rather tedious and is performed with help of the symbolic algebra computer program. Below we list the resulting formulas expressed in a form convenient for the numerical evaluation.

The singular part with the 3P intermediate states is given by (after removing all divergencies)

$$\delta E_{\text{sing}}(^3P) = \left\langle Q' \frac{1}{(E-H)'} T' \right\rangle 2 \langle \vec{I} \cdot \vec{S} \rangle, \quad (\text{C2})$$

where $E \equiv E(^2^3P)$,

$$Q' \equiv Q + \frac{2}{3} \sum_a \left\{ \frac{Z}{r_a}, E - H \right\} = -\frac{2Z}{3} \left(\frac{\vec{r}_1}{r_1^3} \cdot \vec{\nabla}_1 + \frac{\vec{r}_2}{r_2^3} \cdot \vec{\nabla}_2 \right), \quad (\text{C3})$$

$$T' \equiv T - \frac{1}{4} \sum_a \left\{ \frac{Z}{r_a}, E - H \right\} = -\frac{1}{2} \left(E + \frac{Z}{r_1} + \frac{Z}{r_2} - \frac{1}{r} \right)^2 - p_1^i \frac{1}{2r} \left(\delta^{ij} + \frac{r^i r^j}{r^2} \right) p_2^j \\ + \frac{1}{4} \vec{\nabla}_1^2 \vec{\nabla}_2^2 - \frac{Z}{4} \frac{\vec{r}_1}{r_1^3} \cdot \vec{\nabla}_1 - \frac{Z}{4} \frac{\vec{r}_2}{r_2^3} \cdot \vec{\nabla}_2 + \frac{1}{2} \frac{\vec{r}}{r^3} \cdot (\vec{\nabla}_1 - \vec{\nabla}_2), \quad (\text{C4})$$

and it is assumed that the operators T' and Q' act on the function on the right hand side that satisfies the Schrödinger equation with the energy E .

The regular part with the 3P intermediate states is

$$\delta E_{\text{reg}}(^3P) = \sum_{n>2} \frac{1}{E(^2^3P) - E(n^3P)} \left[\langle 2^3\vec{P}|Q|n^3\vec{P} \rangle \langle n^3\vec{P}|\hat{T}|2^3\vec{P} \rangle \left\langle \frac{2}{3} \vec{I} \cdot \vec{L} + I^i L^j (S^i S^j)^{(2)} \right\rangle \right. \\ + \langle 2^3\vec{P}|Q|n^3\vec{P} \rangle \langle n^3\vec{P}|\hat{T}|2^3\vec{P} \rangle \left\langle -\frac{3}{5} I^i S^j (L^i L^j)^{(2)} \right\rangle + \langle 2^3\vec{P}|\hat{Q}|n^3\vec{P} \rangle \langle n^3\vec{P}|T|2^3\vec{P} \rangle \langle \vec{I} \cdot \vec{L} \rangle \\ + \langle 2^3\vec{P}|\hat{Q}|n^3\vec{P} \rangle \langle n^3\vec{P}|\hat{T}|2^3\vec{P} \rangle \left\langle \frac{1}{3} \vec{I} \cdot \vec{S} + \frac{1}{2} I^i S^j (L^i L^j)^{(2)} \right\rangle \\ + \langle 2^3\vec{P}|\hat{Q}|n^3\vec{P} \rangle \langle n^3\vec{P}|\hat{T}|2^3\vec{P} \rangle \left\langle -\frac{3}{10} I^i L^j (S^i S^j)^{(2)} \right\rangle \\ + \langle 2^3\vec{P}|\hat{Q}|n^3\vec{P} \rangle \langle n^3\vec{P}|T|2^3\vec{P} \rangle \left\langle -\frac{6}{5} I^i S^j (L^i L^j)^{(2)} \right\rangle \\ + \langle 2^3\vec{P}|\hat{Q}|n^3\vec{P} \rangle \langle n^3\vec{P}|\hat{T}|2^3\vec{P} \rangle \left\langle -\frac{1}{3} \vec{I} \cdot \vec{L} + \frac{9}{20} I^i S^j (L^i L^j)^{(2)} - \frac{1}{20} I^i L^j (S^i S^j)^{(2)} \right\rangle \\ \left. + \langle 2^3\vec{P}|\hat{Q}|n^3\vec{P} \rangle \langle n^3\vec{P}|\hat{T}|2^3\vec{P} \rangle \left\langle \frac{1}{5} \vec{I} \cdot \vec{S} - \frac{21}{100} I^i S^j (L^i L^j)^{(2)} - \frac{27}{100} I^i L^j (S^i S^j)^{(2)} \right\rangle \right]. \quad (\text{C5})$$

The other parts are

$$\begin{aligned} \delta E^{(1P)} = \sum_n \frac{1}{E(2^3P) - E(n^1P)} & \left[\langle 2^3\bar{P} | Q_A | n^1\bar{P} \rangle \langle n^1\bar{P} | \bar{T}_A | 2^3\bar{P} \rangle \langle \frac{1}{3} \bar{I} \cdot \bar{L} - I^i L^j (S^i S^j)^{(2)} \rangle \right. \\ & \left. + \langle 2^3\bar{P} | \hat{Q}_A | n^1\bar{P} \rangle \langle n^1\bar{P} | \bar{T}_A | 2^3\bar{P} \rangle \langle -\frac{1}{6} \bar{I} \cdot \bar{L} + \frac{9}{20} I^i S^j (L^i L^j)^{(2)} + \frac{1}{20} I^i L^j (S^i S^j)^{(2)} \rangle \right], \end{aligned} \quad (C6)$$

$$\begin{aligned} \delta E^{(3D)} = \sum_n \frac{1}{E(2^3P) - E(n^3D)} & \left[\langle 2^3\bar{P} | \bar{Q} | n^3\hat{D} \rangle \langle n^3\hat{D} | \bar{T} | 2^3\bar{P} \rangle \langle \frac{2}{3} \bar{I} \cdot \bar{S} - \frac{1}{5} I^i S^j (L^i L^j)^{(2)} \rangle \right. \\ & + \langle 2^3\bar{P} | \hat{Q} | n^3\hat{D} \rangle \langle n^3\hat{D} | \hat{T} | 2^3\bar{P} \rangle \langle \frac{2}{9} \bar{I} \cdot \bar{S} + \frac{7}{30} I^i S^j (L^i L^j)^{(2)} - \frac{1}{10} I^i L^j (S^i S^j)^{(2)} \rangle \\ & + \langle 2^3\bar{P} | \hat{Q} | n^3\hat{D} \rangle \langle n^3\hat{D} | \bar{T} | 2^3\bar{P} \rangle \langle -\frac{2}{3} \bar{I} \cdot \bar{L} - \frac{3}{10} I^i S^j (L^i L^j)^{(2)} - \frac{1}{10} I^i L^j (S^i S^j)^{(2)} \rangle \\ & \left. + \langle 2^3\bar{P} | \bar{Q} | n^3\hat{D} \rangle \langle n^3\hat{D} | \hat{T} | 2^3\bar{P} \rangle \langle -\frac{3}{5} I^i L^j (S^i S^j)^{(2)} \rangle \right], \end{aligned} \quad (C7)$$

$$\delta E^{(1D)} = \sum_n \frac{1}{E(2^3P) - E(n^1D)} \langle 2^3\bar{P} | \hat{Q}_A | n^1\hat{D} \rangle \langle n^1\hat{D} | \bar{T}_A | 2^1\bar{P} \rangle \langle -\frac{1}{3} \bar{I} \cdot \bar{L} - \frac{3}{10} I^i S^j (L^i L^j)^{(2)} + \frac{1}{10} I^i L^j (S^i S^j)^{(2)} \rangle, \quad (C8)$$

$$\delta E^{(3F)} = \sum_n \frac{1}{E(2^3P) - E(n^3F)} \langle 2^3\bar{P} | \hat{Q} | n^3\tilde{F} \rangle \langle n^3\tilde{F} | \hat{T} | 2^3\bar{P} \rangle \langle \frac{1}{3} \bar{I} \cdot \bar{S} - \frac{1}{10} I^i S^j (L^i L^j)^{(2)} + \frac{3}{10} I^i L^j (S^i S^j)^{(2)} \rangle. \quad (C9)$$

The matrix elements with the D and F -state wave functions are defined by

$$\langle \vec{\phi} | \vec{Q} | \hat{\psi} \rangle \equiv -i \langle \phi_i | Q_j | \psi_{ij} \rangle = i \langle \psi_{ij} | Q_j | \phi_i \rangle \equiv \langle \hat{\psi} | \vec{Q} | \vec{\phi} \rangle, \quad (C10)$$

$$\langle \vec{\phi} | \hat{Q} | \hat{\psi} \rangle \equiv \epsilon^{ijk} \langle \phi_i | Q_{jl} | \psi_{kl} \rangle = \epsilon^{ijk} \langle \psi_{kl} | Q_{jl} | \phi_i \rangle \equiv \langle \hat{\psi} | \hat{Q} | \vec{\phi} \rangle, \quad (C11)$$

$$\langle \vec{\phi} | \hat{Q} | \tilde{\psi} \rangle \equiv \langle \phi_i | Q_{jk} | \psi_{ijk} \rangle = \langle \psi_{ijk} | Q_{ij} | \phi_k \rangle \equiv \langle \tilde{\psi} | \hat{Q} | \vec{\phi} \rangle, \quad (C12)$$

where $\hat{\psi}$ denotes the odd D wave function,

$$\psi^{ij} = \left(\epsilon^{ikl} r_1^k r_2^l r_1^j + \epsilon^{jkl} r_1^k r_2^l r_1^i \right) f(r_1, r_2, r) \pm (r_1 \leftrightarrow r_2), \quad (C13)$$

and $\tilde{\psi}$ denotes the odd F wave function,

$$\begin{aligned} \psi^{ijk} = & \left[r_1^i r_1^j r_1^k - \frac{r_1^2}{5} (\delta_{ij} r_1^k + \delta_{ik} r_1^j + \delta_{jk} r_1^i) \right] f(r_1, r_2, r) + \frac{1}{3} \left[r_1^i r_1^j r_2^k + r_1^i r_2^j r_1^k + r_2^i r_1^j r_1^k \right. \\ & \left. - \frac{\delta_{ij}}{5} (r_1^2 r_2^k + 2r_1^l r_2^l r_1^k) - \frac{\delta_{ik}}{5} (r_1^2 r_2^j + 2r_1^l r_2^l r_1^j) - \frac{\delta_{jk}}{5} (r_1^2 r_2^i + 2r_1^l r_2^l r_1^i) \right] g(r_1, r_2, r) \pm (r_1 \leftrightarrow r_2). \end{aligned} \quad (C14)$$

All wave functions are real and normalized by $\langle \psi^i | \psi^i \rangle = \langle \psi^{ij} | \psi^{ij} \rangle = \langle \psi^{ijk} | \psi^{ijk} \rangle = 1$.

The second-order corrections listed above are finite. However, some matrix elements are too singular for the direct numerical evaluation and need to be transformed to a more regular form. The regularization method is described in Sec. IV. So, the operator T is transformed by Eq. (32), thus yielding

$$\begin{aligned} & \sum_{n>2} \frac{1}{E(2^3P) - E(n^3P)} \langle 2^3\bar{P} | \bar{Q} | n^3\bar{P} \rangle \langle n^3\bar{P} | T | 2^3\bar{P} \rangle \\ & = \sum_{n>2} \frac{1}{E(2^3P) - E(n^3P)} \langle 2^3\bar{P} | \bar{Q} | n^3\bar{P} \rangle \langle n^3\bar{P} | T' | 2^3\bar{P} \rangle + \langle 2^3\bar{P} | \frac{1}{4} \sum_a \frac{Z}{r_a} \bar{Q} | 2^3\bar{P} \rangle - \langle 2^3\bar{P} | \frac{1}{4} \sum_a \frac{Z}{r_a} | 2^3\bar{P} \rangle \langle 2^3\bar{P} | \bar{Q} | 2^3\bar{P} \rangle. \end{aligned} \quad (C15)$$

We observe that, after the transformation, the singular part of the operator T is absorbed in the first-order matrix element, whereas the second-order correction contains only the (more regular) operator T' .

Similarly, the operator Q^{ij} is transformed by

$$Q^{ij} \equiv Q^{ij} - \{ \delta Q^{ij}, E - H \} = -\frac{Z}{6} \sum_a \left(-\delta^{ij} \frac{r_a^k}{r_a^3} - 3 \delta^{ik} \frac{r_a^j}{r_a^3} - 3 \delta^{jk} \frac{r_a^i}{r_a^3} + 9 \frac{r_a^i r_a^j r_a^k}{r_a^5} \right) \nabla_a^k, \quad (C16)$$

where $E \equiv E(2^3 P)$,

$$\delta Q^{ij} = \frac{1}{6} \sum_a \frac{Z}{r_a} \left(\delta^{ij} - 3 \frac{r_a^i r_a^j}{r_a^2} \right) \quad (\text{C17})$$

and it is assumed that the function on the right hand side of \hat{Q}' satisfies the Schrödinger align with energy E . The second-order matrix elements with Q^{ij} then are transformed by

$$\begin{aligned} & \sum_{n>2} \frac{1}{E(2^3 P) - E(n^3 P)} \langle 2^3 \vec{P} | \hat{Q}' | n^3 \vec{P} \rangle \langle n^3 \vec{P} | \vec{T} | 2^3 \vec{P} \rangle \\ &= \sum_{n>2} \frac{1}{E(2^3 P) - E(n^3 P)} \langle 2^3 \vec{P} | \hat{Q}' | n^3 \vec{P} \rangle \langle n^3 \vec{P} | \vec{T} | 2^3 \vec{P} \rangle + (-i\epsilon^{klm}) \langle 2^3 P_i | \delta Q_{ik} T_l | 2^3 P_m \rangle - \langle 2^3 \vec{P} | \delta \hat{Q} | 2^3 \vec{P} \rangle \langle 2^3 \vec{P} | \vec{T} | 2^3 \vec{P} \rangle, \end{aligned} \quad (\text{C18})$$

and

$$\begin{aligned} & \sum_{n>2} \frac{1}{E(2^3 P) - E(n^3 P)} \langle 2^3 \vec{P} | \hat{Q}' | n^3 \vec{P} \rangle \langle n^3 \vec{P} | T | 2^3 \vec{P} \rangle = \sum_{n>2} \frac{1}{E(2^3 P) - E(n^3 P)} \langle 2^3 \vec{P} | \hat{Q}' | n^3 \vec{P} \rangle \langle n^3 \vec{P} | T' | 2^3 \vec{P} \rangle \\ &+ \langle 2^3 \vec{P} | \frac{1}{4} \sum_a \frac{Z}{r_a} \hat{Q} | 2^3 \vec{P} \rangle - \langle 2^3 \vec{P} | \frac{1}{4} \sum_a \frac{Z}{r_a} | 2^3 \vec{P} \rangle \langle 2^3 \vec{P} | \hat{Q} | 2^3 \vec{P} \rangle + \langle 2^3 \vec{P} | \delta \hat{Q} T' | 2^3 \vec{P} \rangle - \langle 2^3 \vec{P} | \delta \hat{Q} | 2^3 \vec{P} \rangle \langle 2^3 \vec{P} | T' | 2^3 \vec{P} \rangle. \end{aligned} \quad (\text{C19})$$

The operator Q_A is transformed as

$$Q'_A \equiv Q_A + \frac{2}{3} \left\{ \frac{Z}{r_1} - \frac{Z}{r_2}, E - H \right\} = \frac{2Z}{3} \left(-\frac{\vec{r}_1}{r_1^3} \cdot \vec{\nabla}_1 + \frac{\vec{r}_2}{r_2^3} \cdot \vec{\nabla}_2 \right), \quad (\text{C20})$$

where it is assumed that the function on the right hand side of Q'_A satisfies the Schrödinger equation with the energy E . The regularized form of the second-order matrix element then is

$$\begin{aligned} & \sum_n \frac{1}{E(2^3 P) - E(n^1 P)} \langle 2^3 \vec{P} | Q_A | n^1 \vec{P} \rangle \langle n^1 \vec{P} | \vec{T}_A | 2^3 \vec{P} \rangle = \\ & \sum_n \frac{1}{E(2^3 P) - E(n^1 P)} \langle 2^3 \vec{P} | Q'_A | n^1 \vec{P} \rangle \langle n^1 \vec{P} | \vec{T}_A | 2^3 \vec{P} \rangle - \frac{2}{3} \langle 2^3 \vec{P} | \left(\frac{Z}{r_1} - \frac{Z}{r_2} \right) \vec{T}_A | 2^3 \vec{P} \rangle. \end{aligned} \quad (\text{C21})$$
